



# Renal myxoboliosis of *Metynnis hypsauchen* in the Brazilian Amazon: morphological and histopathological aspects

Jhonata Eduard Farias de Oliveira<sup>1</sup>, Rayline Thaimenne Alves Figueredo<sup>2</sup>, Maria do Perpétuo Socorro Progene Vilhena<sup>3</sup>, José Francisco Berrêdo<sup>4</sup>, José Ledamir Sindeaux-Neto<sup>5</sup>, Edilson Matos<sup>5</sup> and Michele Velasco<sup>6\*</sup>

<sup>1</sup>Programa de Pós-graduação em Aquicultura e Recursos Aquáticos Tropicais, Universidade Federal Rural da Amazônia, Belém, Pará, Brazil. <sup>2</sup>Programa de Pós-graduação em Biologia Animal, Universidade Estadual de Campinas, Campinas, São Paulo, Brazil. <sup>3</sup>Universidade Federal Rural da Amazônia, Tomé-Açu, Pará, Brazil. <sup>4</sup>Museu Paraense Emílio Goeldi, Belém, Pará, Brazil. <sup>5</sup>Laboratório de Pesquisa Carlos Azevedo, Universidade Federal Rural da Amazônia, Belém, Pará, Brazil. <sup>6</sup>Universidade Federal Rural da Amazônia, PA-256, 68627-451, Paragominas, Pará, Brazil. \*Author for correspondence. E-mail: michele.velasco.mv@gmail.com

**ABSTRACT.** In their natural habitat, fish are constantly threatened by ichthyoparasites, notably those from the Phylum Cnidaria, Hatschek, 1888, represented by species of the Myxozoa, responsible for infections in fish that cause complications to their health that can lead to death. Among these parasites, the genus *Myxobolus* Butschli, 1882 is responsible for the largest number of infections described in fishes from the Americas. This study describes the morphological and histopathological aspects of parasitism by *Myxobolus* sp. in specimens of *Metynnis hypsauchen*, obtained from the Capim river, in the municipality of IPIXUNA DO PARÁ, Pará, Brazil. During the months of August and March, 2018, 20 animals were captured, euthanized and autopsied. With the aid of a stereomicroscope an external and internal investigation was performed on the animals for the purpose of finding lesions or parasitic cysts, followed by confirmation of infection in Light Microscopy (ML). Cysts and Fragments from parasitized tissues were processed using techniques for histology and Scanning Electron Microscopy (SEM). For histology they were stained with Hematoxylin-Eosin (H-E) and Ziehl-Neelsen and for SEM Micrographs were captured, using equipment from the Museu Paraense Emílio Goeldi. The prevalence of parasitism was 60% (12/20) of the specimens, and the cysts were in the epithelium and lumen of the renal tubules, causing histopathological changes. The characteristics of the parasite spores are those associated with the genus *Myxobolus*, with an ellipsoid format, two polar capsules and a sporoplasm region. It was possible to confirm a high parasite load of *Myxobolus*, with compromised renal functions. This study is the first to describe Myxospore in *Metynnis hypsauchen*.

**Keywords:** Amazon; Serrasalminidae; myxozoan; kidneys.

Received on October 17, 2019.  
Accepted on February 13, 2020.

## Introduction

The Capim River, located in the municipality of IPIXUNA DO PARÁ in the Brazilian Amazon, has an extension of about 600 km of areas. *Metynnis hypsauchen* Müller & Troschel, 1844, Serrasalminidae, popularly known in the Amazon region as “white pacu”, is one of the species that integrates local diversity (Montag, Freitas, Wosiacki, & Barthem, 2008; Garavello & Oliveira, 2014). It is sold in some locations as an ornamental fish (Sánchez Riveiro, García Vásquez, Vásquez Bardales, & Alcántara Bocanegra, 2011). It belongs to the most diverse genus in the family, with 15 species (Boyle & Herrel, 2018; Ota, Daniel, & Jégu, 2016).

The Myxozoa, belonging to the Phylum Cnidaria, Hatschek 1888, are made up of parasitic spores that infect vertebrates and invertebrates (Békési, Székely, & Molnár, 2002; Okamura, Gruhl, & Bartholomew, 2015; Foox & Siddall, 2015). There are approximately 2,600 species described (Okamura, Hartigan, & Naldoni, 2018). This diversity is attributed to the use of fish as intermediate hosts (Holzer et al., 2018). They are found in practically all organs, such as: gills, scales, fins, gallbladder and other vital organs (Lom & Dyková, 2006; Gupta & Kaur, 2017).

Myxobolidae family is the most frequent Myxozoan group found in fish in the Americas (Vidal, Iannacone, Whipps, & Luque, 2017) of which the genus *Myxobolus* Butschli, 1882 is the largest, with more

than 905 species (Eiras, Zhang, & Molnár, 2014; Eiras, Molnár, & Lu, 2005) of which 4 have been described in Brazil, mainly in the Amazon region (Vidal et al., 2017). They have ellipsoid-shaped spores, with two polar pyriform capsules and a binucleated sporoplasm (Lom & Dyková, 2006). Fish are their main vertebrate hosts, but they have also been reported in amphibians and reptiles (Eiras et al., 2005; Eiras et al., 2014). "Whirling disease" is the best known disease, caused by *Myxobolus cerebralis*, resulting from a disoriented ear capsule infection in which the fish chases its own tail in circular movements, as the result of infection in the auditory capsule that leaves it disoriented (Lom & Dyková, 2006; Hoffman, 1990; Faruk, 2018).

This study describes parasitism by *Myxobolus* with a morphological and histopathological description in the teleost fish *Metynnis hypsauchen* collected from the Capim river when it passes through the municipality of Ipixuna do Pará.

## Material and methods

### Fish and sample collection

During the months of August 2018 and March 2019, 20 specimens of *Metynnis hypsauchen* fish were acquired. With the help of fishing gear, they were captured and transported alive in plastic bags with water from their habitat and artificial aeration to the *Laboratório de Pesquisa Carlos Azevedo*, at the *Universidade Federal Rural da Amazônia*, in Belém, Pará, Brazil (License from SISBIO / ICMBio 62276-1).

The animals were anesthetized with tricaine (MS-222) at a concentration of 50 mg L<sup>-1</sup> and then autopsied (License from Animal Use Ethics Committee n° 011/2014) to search for parasites. A stereomicroscope was used, to observe lesions and/or cysts of parasites on the integumentary surface and internal organs. In tissues and organs with probable presence of parasites, small fragments were removed for slide assembly with the addition of a drop of water and observation under a light microscope and with a Differential Interference Contrast Microscope (DIC) (Nomarski) for confirmation.

### Morphometric Analysis

Morphometric data in micrometers (µm), were obtained from mature and fresh spores (mean, standard deviation range in parentheses). According to recommendations from Lom and Arthur (1989) the following variables were analyzed: Length of spores (LS), width of spores (WS), length of polar capsule (PCL) and width of polar capsule (PCW). Findings were compared with those from specimens of *Myxobolus* sp. described in other studies, using Principal Component Analysis (PCA) and the hierarchical method UPGMA, employing the PAST 3.0 software (Hammer, Harper, & Ryan, 2001).

### Histology

Histological processing began by removing parasitized kidney fragments that were fixed in Davidson solution (95% alcohol, formaldehyde, acetic acid and distilled water) for 24 hours and dehydrated in progressive alcohol concentration, then paraffinized and microtomed with 0.5 µm thick sections and finally stained with Hematoxylin-Eosin and Ziehl-Neelsen (Luna, 1968).

### Scanning Electron Microscopy

For analysis with Scanning Electron Microscopy (SEM), the parasitized kidney fragments were fixed in glutaraldehyde 5%, buffered with sodium cacodylate with Ph 7.2 for 12 hours at 4°C. Next, the samples were washed in the same buffering solution and fixed in OsO<sub>4</sub> at 2%, and buffered for 3 hours without temperature change. Later on, they were desiccated in an increasing propylene oxide series and dried to the critical point, metallized with a thin layer of gold and photographed with a Tescan Mira3 scanning electron microscope, with an FEG electron gun (field emission gun), located at the *Centro de Microscopia do Museu Paraense Emílio Goeldi* in Belém, PA.

## Results

### Light microscopy and ultrastructure

In the evaluation using light microscopy, 60% (12/20) of the specimens autopsied presented infection in the kidneys from *Myxobolus* sp. The spores were located in the renal tubules (Figures 1a-1b). They had an

elliptical format, measuring 12.3-12.7 ( $12.5\pm 0.3$ )  $\mu\text{m}$  length and 7.2-7.5 ( $7.3\pm 0.2$ )  $\mu\text{m}$  width and containing sporoplasm (Figure 1c). The polar capsules were the same size and elongated, with 6.1-6.3 ( $6.2\pm 0.2$ )  $\mu\text{m}$  length and 2.79-2.9 ( $2.8\pm 0.07$ )  $\mu\text{m}$  width. The polar filaments presented 8-10 turns (Figure 2). Observations using scanning electronic microscopy, showed spores with two smooth united valves and the suture line region between the valves (Figures 3a – 3c).

The microcut of the kidneys showed cysts, containing spores of *Myxobolus* sp., with typical polar capsules (Figure 4f), located in the mucosa and epithelium of the Proximal Convoluted Tubules (PCT) of the nephron, causing deformation and compression of the cuboidal cells of the epithelium, and the lateral displacement of the lumen (Figures 4 a-f). Some free spores were also found in the renal parenchyma (Figure 4 d). In the Hematoxylin-Eosin stain, mononuclear leucocyte infiltrate was noticed close to the infection site and multifocal necrosis (Figures 4a and c). Melanomacrophagic bodies were also visualized in the PCT wall, with a more prominent coloring (Figure 4b), a typical finding with many infections.

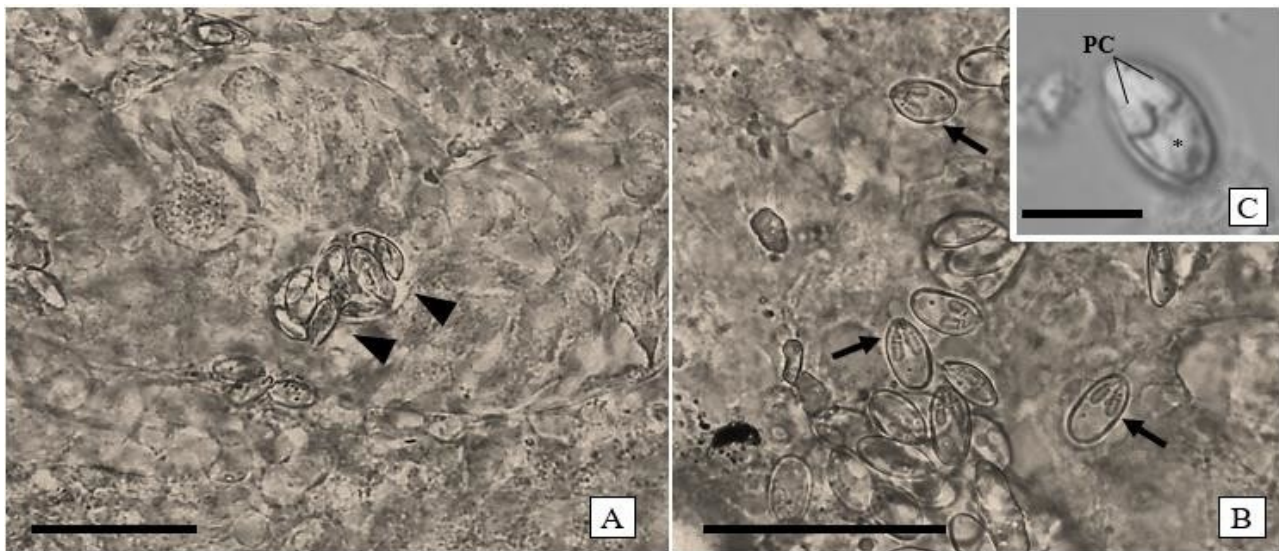


**Figure 1.** Photomicrographs of mature to fresh myxospore of *Myxobolus* sp. infecting the kidneys of *Metynnix hypsauchen*. A and B. Observation of cysts (black arrow point) and spores (arrows). C. Spore observed with Microscopy using Differential Interference Contrast (DIC), notably the polar capsules (PC) and sporoplasm region (\*). Scale bar= 20 $\mu\text{m}$ .

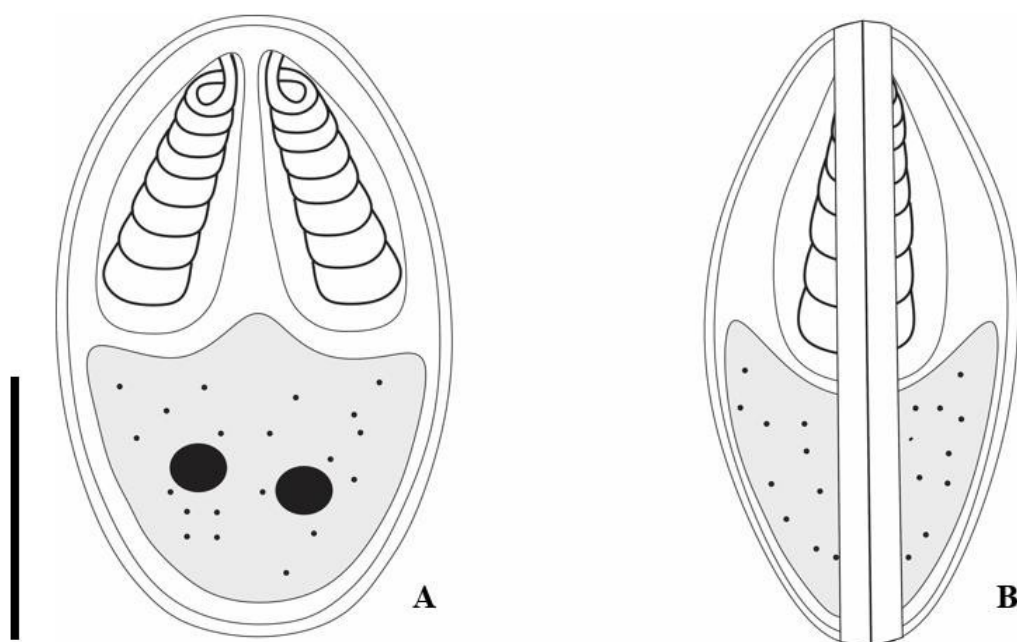


**Figure 2.** Schematic drawing of mature spores of *Myxobolus* sp. A. Front view; B. Side view. Scale bar = 5  $\mu\text{m}$ .

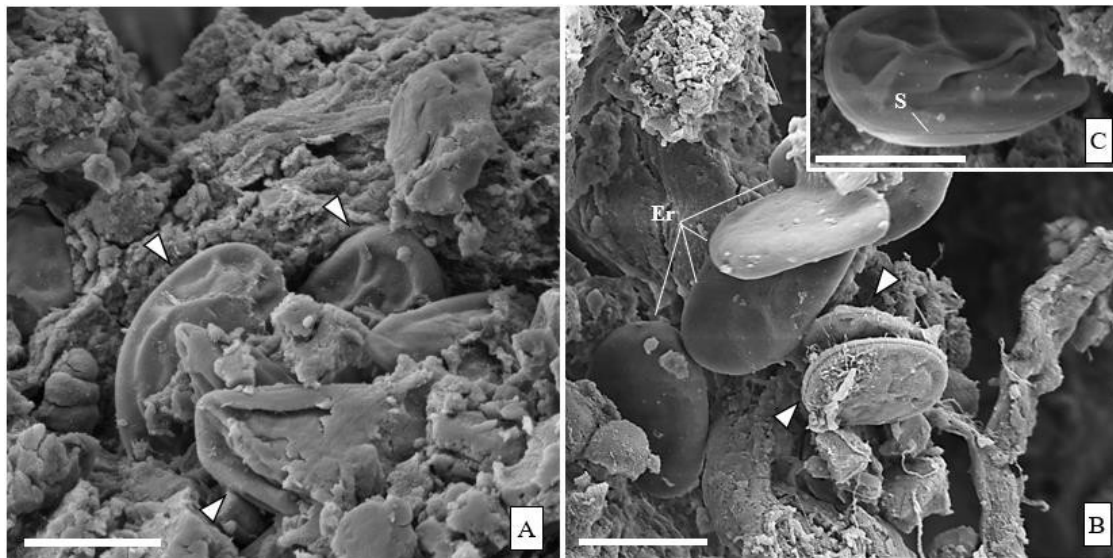


**Figure 3.** Scanning electron micrographs of myxospore of *Myxobolus* sp. infecting the kidneys of *Metynnis hypsauchen*. A and B. Observation of mature myxospores (white arrow point) and with some myxospores close to erythrocytes (Er). C. The suture line of a mature myxospore is highlighted (S). Scale bar= 5μm.

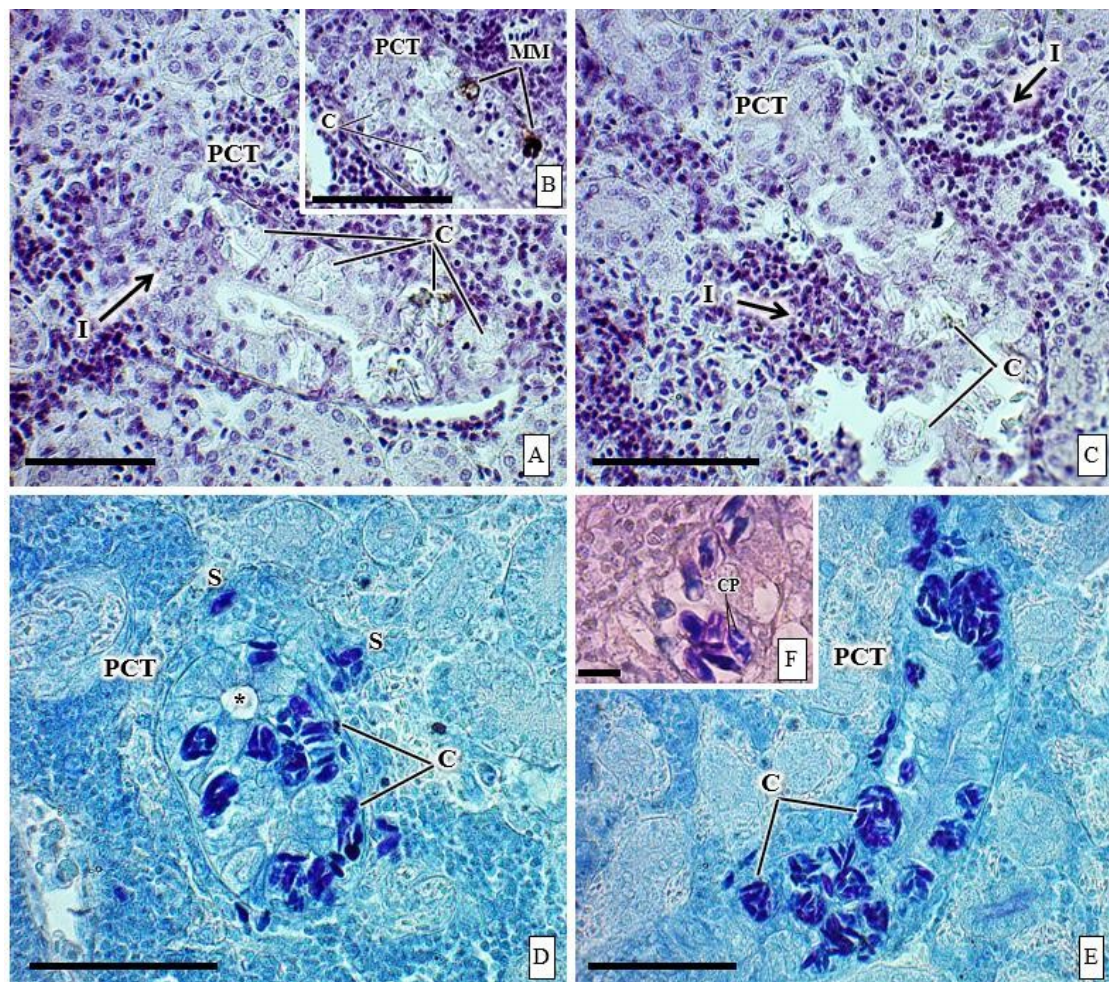


**Figure 4.** Photomicrographs of tissue sections from the kidney of *Metynnis hypsauchen* infected by *Myxobolus* sp., showing longitudinal (A and E) and cross-section cuts (C and D) of proximal convoluted tubules (PCT). A, B and C. Cysts of mature myxospores (C) causing compression and deformation in the cuboid epithelium of the proximal convoluted tubule (PCT). Note the inflammatory mononuclear infiltrate (I) around the infected tubule and the multifocal necrosis area (arrow) and melanomacrophages (MM) close to the infection site. Hematoxylin and Eosin. D and E. Cysts of mature myxospores in the cuboid epithelium of the proximal convoluted tubules (PCT), causing deformation and displacement of the lumen (\*) to the side of the tubule. Observation of free myxospores in the renal parenchyma (S). Scale bar= 50μm. F. Detail of the myxospore found in the polar capsules (CP). Scale bar= 10μm.

The morphometric analysis demonstrated that the *Myxobolus* sp. spore, was significantly different from spores of the majority of the species described at different infection sites, with *M. metynniss* found in the orbicular tissue of *Metynniss argenteus* and *M. aureus* causing liver infection in *Salminus brasiliensis*, were the closest (Figure 6), in length and width of spore (Table 1). However, it is not possible to assert the similarity with both species, due to the negative relationship in the ordering and Euclidean distance axes (Figures 5 and 6).

**Table 1.** Comparison of morphologic data between spores of *Myxobolus* spp. basead on 20 spores measurements. All measured in micrometers.

Species	Spore		Polar Capsule		Filament Coils	Host/Infection Site	References
	Length	Width	Length	Width			
<i>Myxobolus</i> sp.	12.3-12.7 (12.5±0.3)	7.2-7.5 (7.3±0.2)	6.1-6.3 (6.2±0.2)	2.79-2.9 (2.8±0.07)	8-10	<i>Metynniss hypsauchen</i> , kidneys	Present Study
<i>M. maculatus</i>	21 (19.7-23)	8.9 (7.9-9.5)	12.7 (11.8-13.8)	3.2 (3-3.6)	14-15	<i>Metynniss maculatus</i> , kidneys	Casal, Matos, & Azevedo (2002)
<i>M. serrasalmi</i>	(14.8±3.1)	(8.6±3.9)	(7.7±2.3)	(3.1±0.9)	-	<i>Serrasalmus rhombeus</i> , kidneys	Walliker (1969)
<i>M. hilarii</i>	9.8 - 13.4 (11.5±0.8)	9.7 - 12.4 (11±0.7)	6 - 7.2 (6.5±0.4)	3.6 - 5.3 (4±0.2)	5-7	<i>Brycon hilarii</i> , kidneys	Capodifoglio, Adriano, Milanin, Silva, & Maia (2016)
<i>M. tapajosi</i>	15 (13.5-17)	10.7 (9.6-11.4)	5.8 (4.6-7.1)	3 (2.3-3.8)	6-7	<i>Brachyplatystoma rousseauxii</i> , branchial filaments	Zatti et al. (2018)
<i>M. aureus</i>	(12.6±0.5)	(8.3±0.3)	(5.7±0.3)	(2.9±0.2)	7-8	<i>Salminus brasiliensis</i> , liver	Carriero, Adriano, Silva, Ceccarelli, & Maia (2013)
<i>M. brycon</i>	6.5-7.2 (6.9±0.6)	3.9-4.8 (4.2±0.5)	3.8-4.7 (4.2±0.6)	1.7-2.5 (1.9±0.6)	8-9	<i>Brycon hilarii</i> , gills	Azevedo, Casal, Marques, Silva, & Matos (2011)
<i>M. piraputangae</i>	(10.1±0.5)	(8.7±0.5)	(5.2±0.4)	(3.0±0.3)	4-5	<i>Brycon hilarii</i> , kidneys	Carriero et al. (2013)
<i>M. metynniss</i>	13.1 (12.9-13.5)	7.8 (7.5-8.3)	5.2 (5.0-5.5)	3.2 (3.0-3.6)	8-9	<i>Metynniss argenteu</i> , orbicular tissue	Casal, Matos, & Azevedo (2006)
<i>M. marajoensis</i>	10.9 (10-11.6)	5.1 (4.2-5.4)	5.2 (5.3± 0.6)	1.5 (1.6±0.36)	-	<i>Rhamdia quelen</i> , Intestine	Abrunhosa, Sindeaux-Neto, Santos, Hamoy, & Matos (2017)
<i>M. matosi</i>	9.1-10.8 (9.6±0.4)	6.5-7.6 (7.0±0.3)	3.3-5.0 (4.3±0.4)	1.6-2.2 (1.9±0.1)	-	<i>Colossoma macropomum</i> , operculum	Capodifoglio, Adriano, Silva, & Maia (2019)

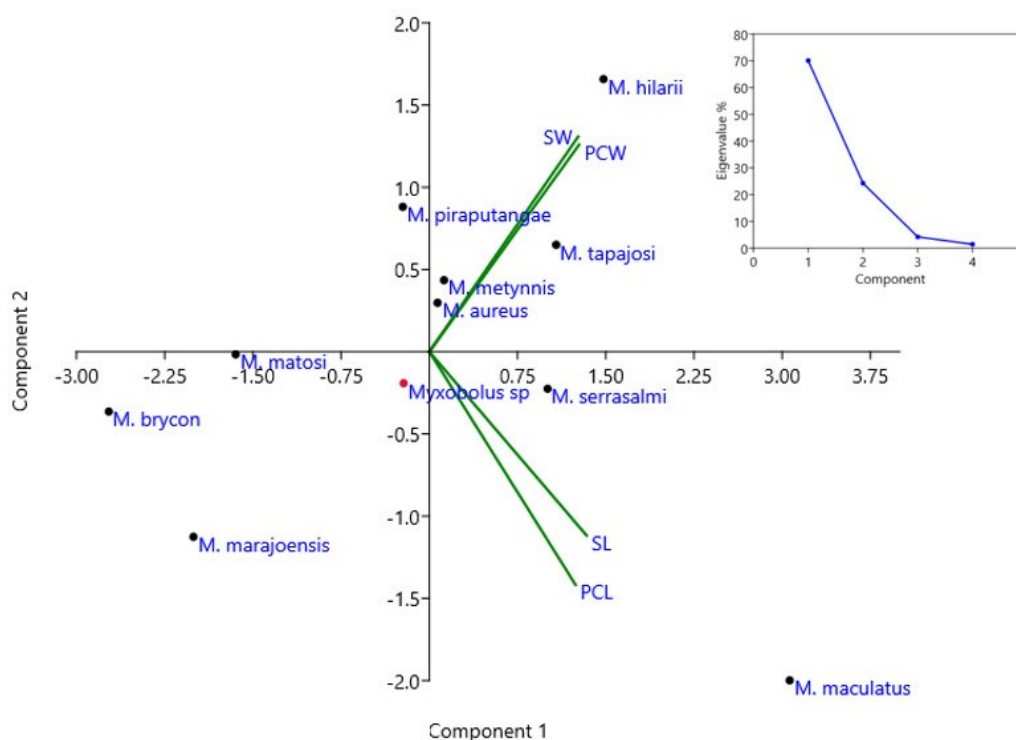


**Figure 5.** Principal Component Analysis (PCA). Correlation of morphometric parameters for the species. Length of spore (SL), Width of spore (SW), Length of Polar Capsule (PCL), Width of Polar Capsule (PCW).

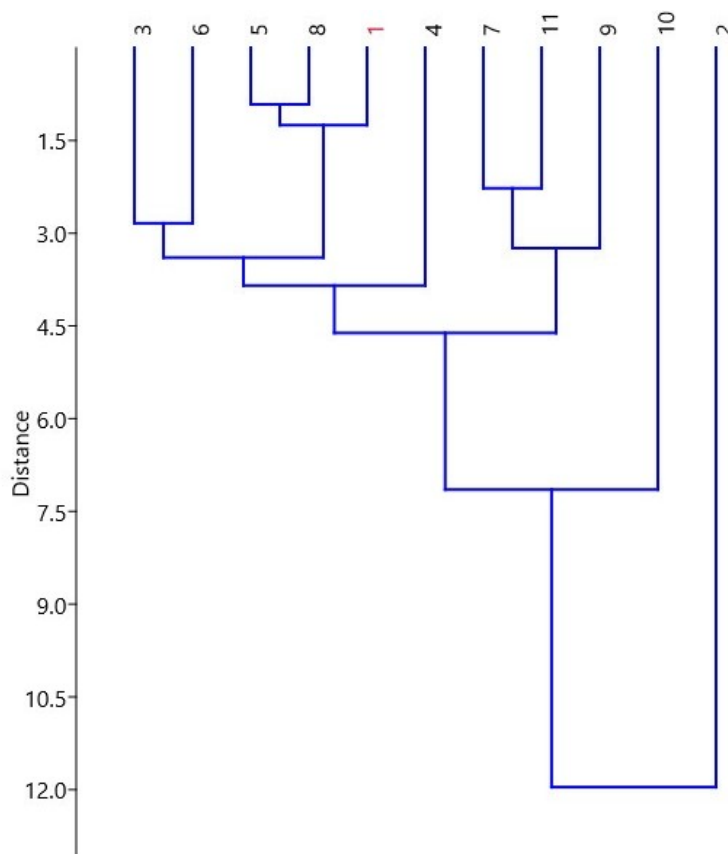


**Figure 6** Similarity dendrogram (UPGMA) between spores of *Myxobolus* spp. 1- *Myxobolus* sp.; 2- *M. maculatus*; 3- *M. serrasalmi*.; 4- *M. hilarii*; 5- *M. metynnis*; 6- *M. tapajosi*; 7- *M. matosi*; 8- *M. aureus*; 9- *M. marajoensis*; 10- *M. brycon*; 11- *M. piraputangae*.

## Discussion

In this study, the prevalence of *Myxobolus* sp. in the renal tubules was 60% (12/20) in *Metynnis hypsauchen* kidneys. When compared with *M. metynnis* (Casal et al., 2006), *M. tapajosi* (Zatti et al., 2018), *M. matosi* (Capodifoglio et al., 2019) and *M. niger* (Mathews, Maia, & Adriano, 2016), species described for the north of Brazil, which respectively presented 40%, 23.5%, 20%, and 13.7% of parasite prevalence, the species studied for this paper presented a higher incidence.

The morphometric analysis demonstrated that the *Myxobolus* sp. spore, was significantly different from that of the majority of the species described at different infection sites, with *M. metynnis* (Casal et al., 2006) found in the orbicular tissue of *Metynnis argenteus* and *M. aureus* (Carriero et al., 2013) causing liver infection in *Salminus brasiliensis*, were the closest (Figure 6), in length and width of spore (Table 1). However, it is not possible to assert a similarity with both species, due to the negative relationship in the ordering and Euclidean distance axes (Figures 5 and 6).

In terms of histopathological findings, they were similar to those from other studies, in which asynchronous spore development led to the compression and degeneration of the tubular cells, leading to a change in lumen size (Capodifoglio et al., 2016; Casal et al., 2002; Abruñhosa, Sindeaux-Neto, Hamoy, & Matos, 2018). There is also a variation in the degree of pathogenicity; in some cases, there was hyaline degeneration, glomerular congestion, cellular edema and formation of a connective capsule around the spores, as reported in kidney infections in the pacu species *Piaractus mesopotamicus* (Manrique, Figueiredo, Belo, Martins, & Molnár, 2017; Campos, Moraes, & Moraes, 2008).

In Hematoxylin-eosin, melanomacrophage cells were observed in the wall of the proximal contorted tubule (Figure 3b), indicating an immune response by the host to the parasitic agent (Agius & Roberts, 2003; Yokoyama, Ogawa, & Wakabayashi, 1995). According to Molnár (2007) some species of Myxozoa have a form of infection characterized by the prevalence of several spores, mainly in the kidney interstitium coming from the bloodstream, which are phagocytosed, stored and destroyed by melanomacrophages, and are regularly seen. *Myxobolus cyprini*, is an example of a species that produces spores in the skeletal muscles and in several organs, and as these mature, they are transported to the kidneys where they are eliminated or

are retained to be destroyed by macrophages (Molnar & Gayer, 1985). Manrique et al. (2017) Found *Myxobolus* spores with structural deformations within the melanomacrophage centers.

This type of infection described is the one most similar to that reported in this paper, although we did not find melanomacrophages phagocytosing and destroying the spores, and the morphological comparison did not correspond to other species described in other organs, which made it difficult to determine the site of origin of the spore. Baki et al. (2015) note that this is the main problem found in infections by myxozoans identifying if the kidneys are the original site of infection or merely a storage point for bloodstream-borne spores.

The inflammatory process revealed in this study is attributed to mononucleated cells due to the small number of melanomacrophages, which does not characterize typical acute infections caused by these cells. Necrotic areas also contribute to inflammation; according to Maftuch et al. (2018), they provide the function of increasing the inflammatory response locally and in nearby regions.

## Conclusion

*Metynnis hypsauchen* is an important ornamental fish species sold by several South American countries. Because of that, these histopathological results are important for understanding the effects of parasitism by *Myxobolus* in the kidneys. We emphasize that this is the first description of Myxosporidia in this host.

## Acknowledgements

The authors thank the *Coordenação de Aperfeiçoamento de Pessoal de Nível Superior (CAPES)* and the *Laboratório de Pesquisa Carlos Azevedo* and the *Centro de Microscopia Eletrônica do Museu Paraense Emílio Goeldi*, for all of their structural support in carrying out the experiments.

## References

- Abrunhosa, J., Sindeaux-Neto, J. L., Hamoy, I., & Matos, E. R. (2018). A new species of Myxosporidia, *Henneguya quelen*, from silver catfish *Rhamdia quelen* (Siluriforme: Pimelodidae) in the Amazonian region. *Parasitology Research*, 117(12), 3809–3820. doi:10.1007/s00436-018-6086-1
- Abrunhosa, J., Sindeaux-Neto, J. L., Santos, Â. K., Hamoy, I., & Matos, E. (2017). *Myxobolus marajoensis* sp. n. (Myxosporidia: Myxobolidae), parasite of the freshwater catfish *Rhamdia quelen* from the Brazilian Amazon region. *Brazilian Journal of Veterinary Parasitology*, 26(4), 465–471. doi:10.1590/S1984-29612017067
- Agius, C., & Roberts, R. J. (2003). Melano-macrophage centres and their role in fish pathology. *Journal of Fish Diseases*, 26(9), 499–509. doi:10.1046/j.1365-2761.2003.00485.x
- Azevedo, C., Casal, G., Marques, D., Silva, E., & Matos, E. (2011). Ultrastructure of *Myxobolus brycon* n. sp. (Phylum Myxozoa), parasite of the piraputanga fish *Brycon hilarii* (Teleostei) from Pantanal (Brazil). *The Journal of Eukaryotic Microbiology*, 58(2), 88–93. doi:10.1111/j.1550-7408.2010.00525.x
- Baki, A. A. S. A., Haleem, H. M. A., Sakran, T., Zayed, E., Ibrahim, K. E., & Al-Quraishy, S. (2015). Two *Myxobolus* spp. infecting the kidney of Nile tilapia (*Oreochromis niloticus*) in the River Nile at Beni-Suef governorate, Egypt, and the associated renal changes. *Parasitology Research*, 114(3), 1107–1112. doi:10.1007/s00436-014-4282-1
- Békési, L., Székely, C., & Molnár, K. (2002). Atuais conhecimentos sobre Myxosporidia (Myxozoa), parasitas de peixes. Um estágio alternativo dos parasitas no Brasil. *Brazilian Journal of Veterinary Research and Animal Science*, 39(5), 271–276. doi: 10.1590/S1413-95962002000500010
- Boyle, K. S., & Herrel, A. (2018). Neurocranium shape variation of piranhas and pacus (Characiformes: Serrasalminae) in association with ecology and phylogeny. *Biological Journal of the Linnean Society*, 125(1), 93–114. doi:10.1093/BIOLINNEAN/BLY092
- Campos, C. M., Moraes, J. R. E., & Moraes, F. R. D. (2008). Histopatologia de fígado, rim e baço de *Piaractus mesopotamicus*, *Prochilodus lineatus* e *Pseudoplatystoma fasciatum* parasitados por myxosporídios, capturados no Rio Aquidauana, Mato Grosso do Sul, Brasil. *Revista Brasileira de Parasitologia Veterinária*, 17(4), 200–205. doi:10.1590/s1984-29612008000400006

- Capodifoglio, K. R. H., Adriano, E. A., Milanin, T., Silva, M. R. M., & Maia, A. A. M. (2016). Morphological, ultrastructural and phylogenetic analyses of *Myxobolus hilarii* n. sp. (Myxozoa, Myxosporea), a renal parasite of farmed *Brycon hilarii* in Brazil. *Parasitology International*, *65*(3), 184–190. doi:10.1016/j.parint.2015.12.006
- Capodifoglio, K. R. H., Adriano, E. A., Silva, M. R. M., & Maia, A. A. M. (2019). The resolution of the taxonomic dilemma of *Myxobolus colossomatis* and description of two novel myxosporeans species of *Colossoma macropomum* from Amazon basin. *Acta Tropica*, *191*, 17–23. doi:10.1016/j.actatropica.2018.12.026
- Carriero, M. M., Adriano, E. A., Silva, M. R. M., Ceccarelli, P. S., & Maia, A. A. M. (2013). Molecular phylogeny of the *Myxobolus* and *Henneguya* genera with several new South American species. *PLoS One*, *8*(9), e73713. doi:10.1371/journal.pone.0073713
- Casal, G., Matos, E., & Azevedo, C. (2002). Ultrastructural data on the spore of *Myxobolus maculatus* n. sp. (Phylum Myxozoa), parasite from the Amazonian fish *Metynnis maculatus* (Teleostei). *DAO - Diseases of Aquatic Organisms*, *51*(2), 107–112. doi:10.3354/dao051107
- Casal, G., Matos, E., & Azevedo, C. (2006). A new myxozoan parasite from the Amazonian fish *Metynnis argenteus* (Teleostei, Characidae): light and electron microscope observations. *Journal of Parasitology*, *92*(4), 817–821. doi:10.1645/ge-750r.1
- Eiras, J. C., Molnár, K., & Lu, Y. S. (2005). Synopsis of the species of *Myxobolus* Bütschli, 1882 (Myxozoa: Myxosporea: Myxobolidae). *Systematic Parasitology*, *61*(1), 1–46. doi:10.1007/s11230-004-6343-9
- Eiras, J. C., Zhang, J., & Molnár, K. (2014). Synopsis of the species of *Myxobolus* Bütschli, 1882 (Myxozoa: Myxosporea, Myxobolidae) described between 2005 and 2013. *Systematic Parasitology*, *88*(1), 11–36. doi:10.1007/s11230-014-9484-5
- Faruk, M. A. R. (2018). Fish parasite: infectious diseases associated with fish parasite. In M. L. Bari & K. Yamazaki (Eds.), *Seafood Safety and Quality* (p. 144–165). Boca Raton: CRC Press.
- Foxx, J., & Siddall, M. E. (2015). The road to cnidaria: history of phylogeny of the Myxozoa. *Journal of Parasitology*, *101*(3), 269–274. doi:10.1645/14-671.1
- Garavello, J. C., & Oliveira, A. K. (2014). Ichthyological overview and remarks on freshwater fishes from Capim river, lower Amazon basin, Brazil. *Open Journal of Ecology*, *4*(13), 797–806. doi:10.4236/oje.2014.413068
- Gupta, A., & Kaur, H. (2017). Record of new host, site of infection and locality of two *Myxobolus* infecting freshwater fishes in Ranjit Sagar wetland of Punjab (India). *International Journal of Biology Research*, *2*(4), 6–11. doi:10.22271/biology
- Hammer, Ø., Harper, D. A. T., & Ryan, P. D. (2001). PAST: paleontological statistics software package for education and data analysis. *Palaeontologia Electronica*, *4*(1), 1–9.
- Hoffman, G. L. (1990). *Myxobolus cerebralis*, a worldwide cause of salmonid whirling disease. *Journal of Aquatic Animal Health*, *2*(1), 30–37. doi:10.1577/1548-8667(1990)002<0030:MCAWCO>2.3.CO;2
- Holzer, A. S., Sojková, P. B., Torrijos, A. B., Lövy, A., Hartigan, A., & Fiala, I. (2018). The joint evolution of the Myxozoa and their alternate hosts: a cnidarian recipe for success and vast biodiversity. *Molecular Ecology*, *27*(7), 1651–1666. doi:10.1111/mec.14558
- Lom, J., & Arthur, J. R. (1989). A guideline for the preparation of species descriptions in Myxosporea. *Journal of Fish Diseases*, *12*(2), 151–156. doi:10.1111/j.1365-2761.1989.tb00287.x
- Lom, J., & Dyková, I. (2006). Myxozoan genera: definition and notes on taxonomy, life-cycle terminology and pathogenic species. *Folia Parasitologica*, *53*(1), 1–36. doi:10.14411/fp.2006.001
- Luna, L. G. (1968). *Manual of histologic staining methods of the Armed Forces Institute of Pathology*. New York, NY: Blakiston Division.
- Maftuch, M., Sanoesi, E., Farichin, I., Saputra, B. A., Ramdhani, L., Hidayati, S., ... Prihanto, A. A. (2018). Histopathology of gill, muscle, intestine, kidney, and liver on *Myxobolus* sp.-infected Koi carp (*Cyprinus carpio*). *Journal of Parasitic Diseases*, *42*(1), 137–143. doi:10.1007/s12639-017-0955-x
- Manrique, W. G., Figueiredo, M. A. P., Belo, M. A. A., Martins, M. L., & Molnár, K. (2017). *Myxobolus* sp. and *Henneguya* sp. (Cnidaria: Myxobolidae) natural co-infection in kidney of *Piaractus mesopotamicus* (Characiformes: Serrasalminidae). *Parasitology Research*, *116*(9), 1–16. doi:10.1007/s00436-017-5571-2

- Mathews, P. D., Maia, A. A. M., & Adriano, E. A. (2016). Morphological and ultrastructural aspects of *Myxobolus niger* n. sp. (Myxozoa) gill parasite of *Corydoras melini* (Siluriformes: Callichthyidae) from Brazilian Amazon. *Acta Tropica*, *158*, 214–219. doi:10.1016/j.actatropica.2016.03.016
- Molnár, K. (2007). Site preference of myxozoans in the kidneys of Hungarian fishes. *Diseases of Aquatic Organisms*, *78*(1), 45–53. doi:10.3354/dao01827
- Molnar, K., & Gayer, É. K. (1985). The pathogenicity and development within the host fish of *Myxobolus cyprini* Doflein, 1898. *Parasitology*, *90*(3), 549–555. doi:10.1017/S0031182000055530
- Montag, L. F. A., Freitas, T. M. S., Wosiacki, W. B., & Barthem, R. B. (2008). Os peixes da Floresta Nacional de Caxiuanã (municípios de Melgaço e Portel, Pará - Brasil). *Boletim do Museu Paraense Emílio Goeldi – Ciências Naturais*, *3*(1), 11–34. doi:10.5123/s1981-81142008000100002
- Okamura, B., Gruhl, A., & Bartholomew, J. L. (2015). An introduction to Myxozoan evolution, ecology and development. In B. Okamura, A. Gruhl & J. L. Bartholomew (Eds.), *Myxozoan evolution, ecology and development* (p. 1–441). Cham, SW: Springer International Publishing.
- Okamura, B., Hartigan, A., & Naldoni, J. (2018). Extensive uncharted biodiversity: the parasite dimension. *Integrative and Comparative Biology*, *58*(6), 1132–1145. doi:10.1093/icb/icy039
- Ota, R. P., Daniel, L. H. R. P., & Jégu, M. (2016). A new Silver Dollar species of *Metynnis* Cope, 1878 (Characiformes: Serrasalminidae) from Northwestern Brazil and Southern Venezuela. *Neotropical Ichthyology*, *14*(4), e160023. doi:10.1590/1982-0224-20160023
- Sánchez Riveiro, H., García Vásquez, A., Vásquez Bardales, J., & Alcántara Bocanegra, F. (2011). *Peces ornamentales amazónicos: catálogo 2011*. Iquitos, PE: IIAP.
- Vidal, L. P., Iannacone, J., Whipps, C. M., & Luque, J. L. (2017). Synopsis of the species of Myxozoa Grassé, 1970 (Cnidaria: Myxosporidia) in the Americas. *Neotropical Helminthology*, *11*(2), 413–511.
- Walliker, D. (1969). Myxosporidia of some Brazilian freshwater fishes. *The Journal of Parasitology*, *55*(5), 942–948. doi:10.2307/3277155
- Yokoyama, H., Ogawa, K., & Wakabayashi, H. (1995). *Myxobolus cultus* n. sp. (Myxosporidia: Myxobolidae) in the goldfish *Carassius auratus* transformed from the Actinosporidian stage in the Oligochaete *Branchiura sowerbyi*. *The Journal of Parasitology*, *81*(3), 446–451. doi:10.2307/3283830
- Zatti, S. A., Atkinson, S. D., Maia, A. A. M., Corrêa, L. L., Bartholomew, J. L., & Adriano, E. A. (2018). Novel *Myxobolus* and *Ellipsomyxa* species (Cnidaria: Myxozoa) parasiting *Brachyplatystoma rousseauxii* (Siluriformes: Pimelodidae) in the Amazon basin, Brazil. *Parasitology International*, *67*(5), 612–621. doi:10.1016/j.parint.2018.06.005